SUPPORTING INFORMATION

Consumption of H_2S from Our Daily diet: Determination by a Simple Chemosensing Method

Ayndrila Ghosh‡, Sujoy Das‡, Himadri S. Sarkar, Shampa Kundu, Prithidipa Sahoo*

Department of Chemistry, Visva-Bharati University, Santiniketan, 731235, W.B., India

*Corresponding author. E-mail: prithidipa@hotmail.com

‡These authors contributed equally.

Table S1. Performance Comparison of Existing Methods and Present Methods based on azide reduction mechanism for Determination of H_2S.

Analytes	Sensor type	Detection limit(µM)	Detection medium	Detection method	Detection state	Sensitivity & Selectivity	Response Time	Estimation in samples	Reference
H_2S	**Napthalimide**	**0.066**	**Neutral**	**Naked eye UV-Vis Fluorescence**	**Liquid Gas**	**High**	**25 sec**	**Foods from daily diet**	**Current method**
H_2S NO NO_2^-	Aza-BODIPY	14.67	Neutral	Naked eye UV-Vis Fluorescence	Liquid	High	30 sec	nd	Anal. Chem. 2014, **86**, 9335−9342.
H_2S	1,8-Napthalimide	nd	Neutral	Fluorescence	Liquid	High	45-60 min	nd	Anal. Chem. 2016, **88**, 9213−9218.
H_2S	D-aminoluciferin	0.1	Neutral	Fluorescence	Liquid	High	60 min	nd	Anal. Chem. 2015, **87**, 11325−11331.
H_2S	Carbon dots-Naphthalimide-azide	0.010	Neutral	UV-Vis Fluorescence	Liquid	High	15 min	nd	Chem. Commun., 2013, **49**, 403-405.
H_2S	Hydrosulfide Naphthalimide	1-10	Neutral	Fluorescence	Liquid	Moderate	45-90 min	nd	Chem. Commun., 2012, **48**, 4767–4769.
H_2S	Coumarin–benzopyrylium	0.22	Neutral	Naked eye UV-Vis Fluorescence	Liquid	High	~1 min	nd	AnalyticaChimicaActa 2015, **859**, 59–65.
H_2S	Dicyanomethylene-4H-chromene	nd	Neutral	Naked eye UV-Vis Fluorescence	Liquid	High	2 min	nd	Dyes and Pigments. 2013, **98**, 367-371

H_2S	Dansylazide	1	Neutral	UV-Vis Fluorescence	Liquid	High	15 min	nd	Angew. Chem. Int. Ed. 2011, **50**, 9672 –9675
H_2S	Imidazole	0.435	Neutral	UV-Vis Fluorescence	Liquid	High	20-30 min	nd	Biochemistry 2014, **53**, 5966−5974.
H_2S, NO	Rhodamine	nd	Neutral	Fluorescence	Liquid	High	25 min	nd	Chem. Commun., 2015, **51**, 4414—4416
H_2S	Rhodamine	5-10	Neutral	Fluorescence	Liquid	High	60 min	nd	J. Am. Chem. Soc. 2011, **133**, 10078–10080.
H_2S	*p*-azidophenylalanine	<50	Neutral	Fluorescence	Liquid	Moderate	12 hrs	nd	J. Am. Chem. Soc. 2012, 134, 9589−9592
H_2S	Coumarin	nd	Neutral	Fluorescence	Liquid	nd	60 min	nd	J. Am. Chem. Soc. 2015, 137, 15330−15336
H_2S	Rhodamine	0.125-0.5	Neutral	Fluorescence	Liquid	High	60 min	nd	PNAS 2013, 110 , 7131–7135
H_2S	Napthalimide	<0.3	Neutral	Naked eye UV-Vis Fluorescence	Liquid	High	40-80 min	nd	Scientific reports. 2016, 26203
H_2S	Dicyanomethylenedihydrofuran	nd	Neutral	Naked eye UV-Vis Fluorescence	Liquid	High	60 min	nd	Tetrahedron Letters 54 (2013) 2980–2982
H_2S	7-Nitrobenz-2-oxa-1,3-diazole	0.68	Neutral	Naked eye UV-Vis Fluorescence	Liquid	High	5 min	nd	Tetrahedron 2013,69, 867-870

1. NMR Studies:

^{1}H NMR of Compound 1in $CDCl_3$:

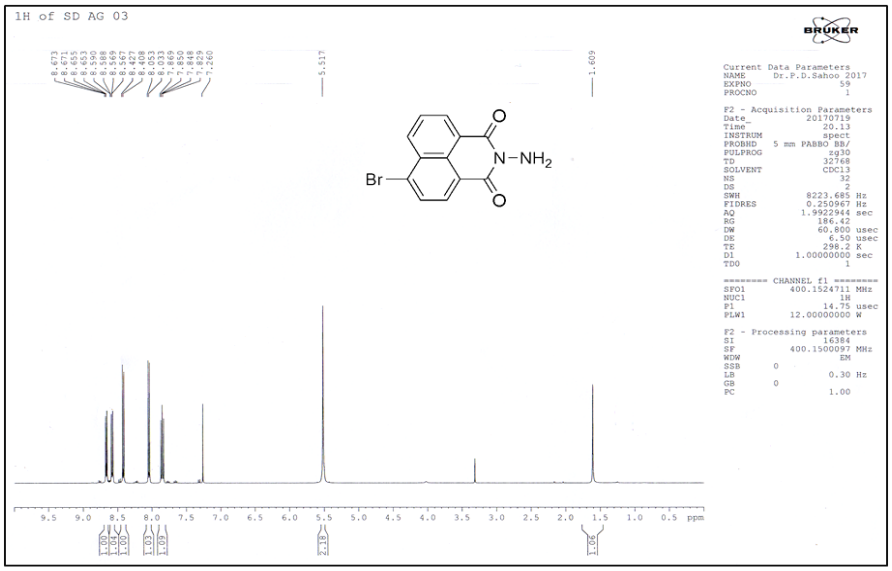

Figure S1. ^{1}H NMR of **Compound 1** in $CDCl_3$

^{1}H NMR of Compound 2 in $CDCl_3$:

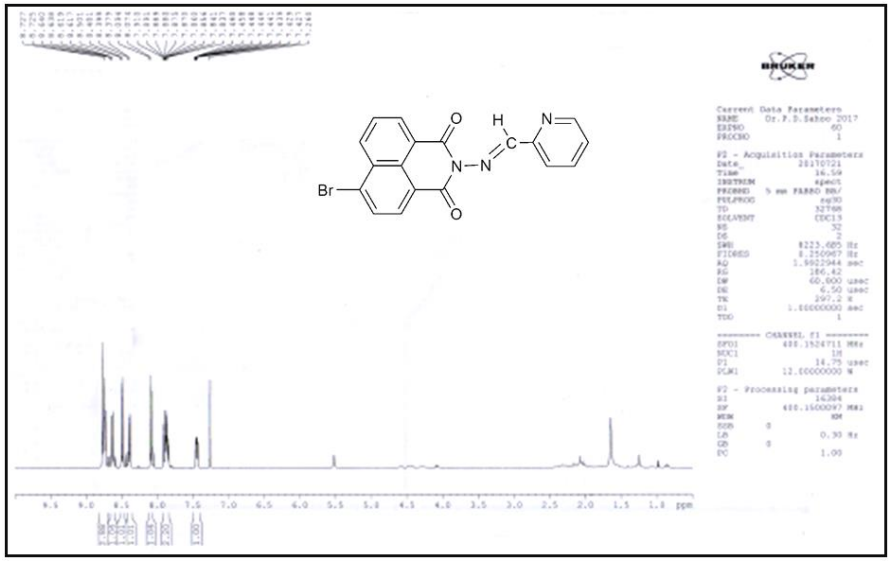

Figure S2.^{1}H NMR of **Compound 2** in $CDCl_3$ (400 MHz).

^{1}H NMR of PN-N_3 in DMSO-d_6:

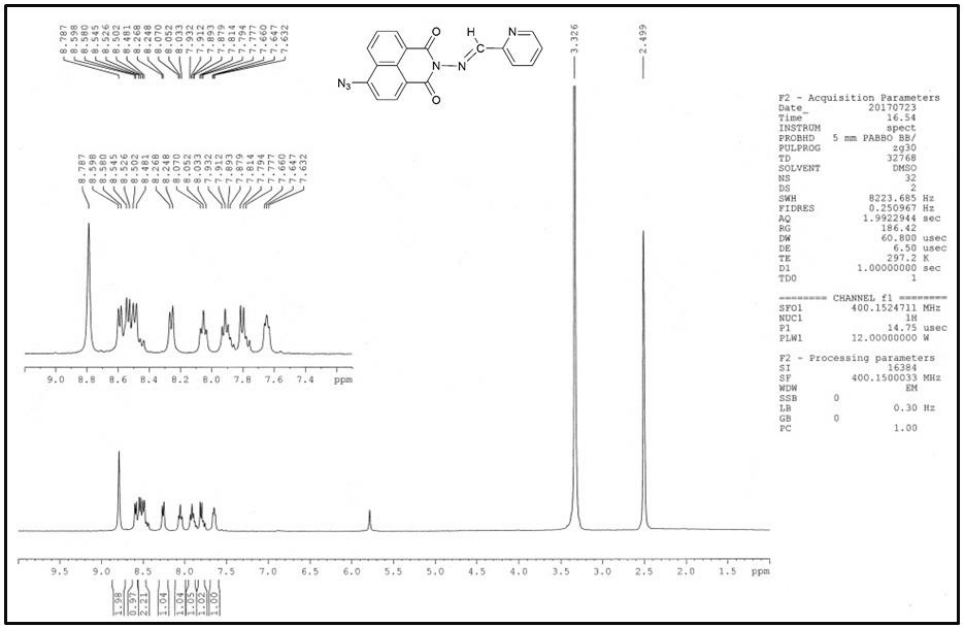

Figure S3. ^{1}H NMR of **PN-N_3** in DMSO-d_6 (400 MHz).

^{13}C NMR of PN-N_3 in DMSO-d_6:

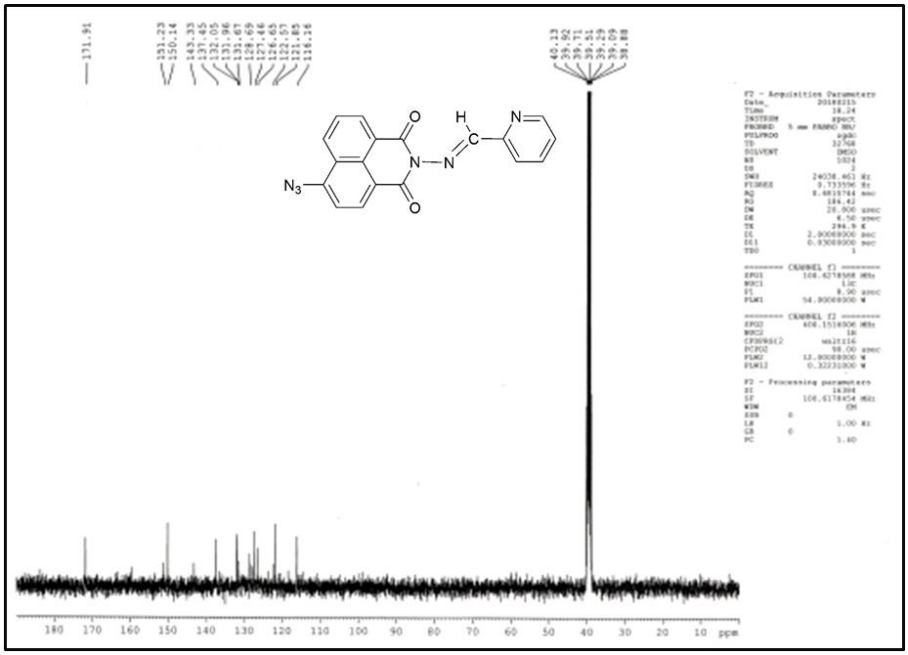

Figure S4.^{13}C NMR of **PN-N_3** in DMSO-d_6 (400 MHz)

2. Mass spectrum of PN-N_3:

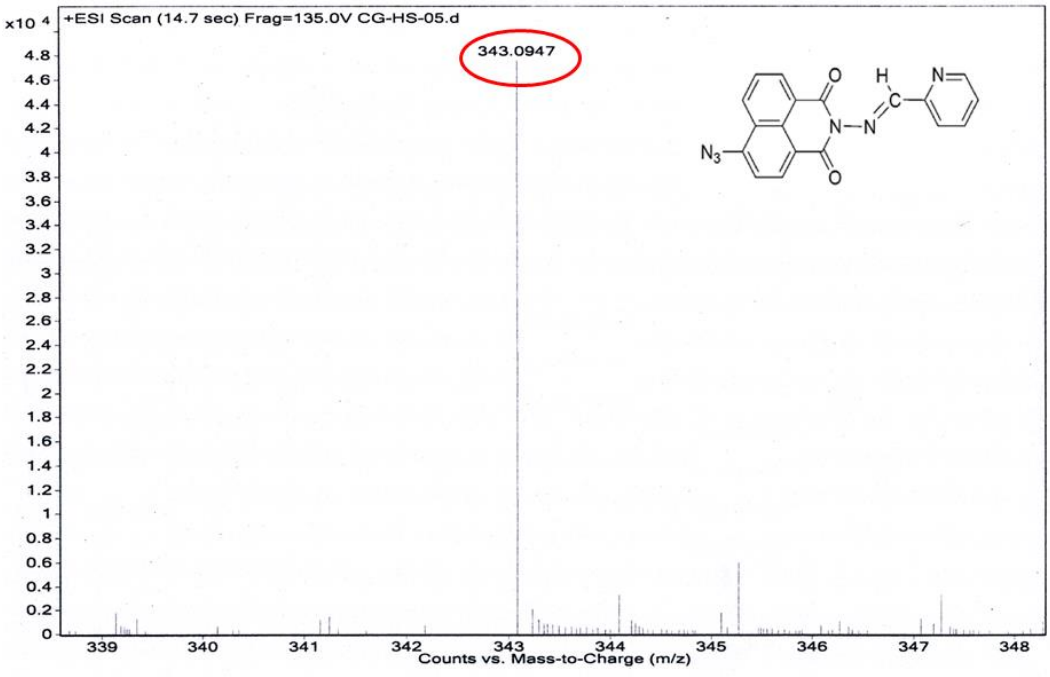

Figure S5. MALDI-TOF MS of **PN-N_3**.

3. Dependence of the absorbance of PN-N_3 on the concentration of H_2S:

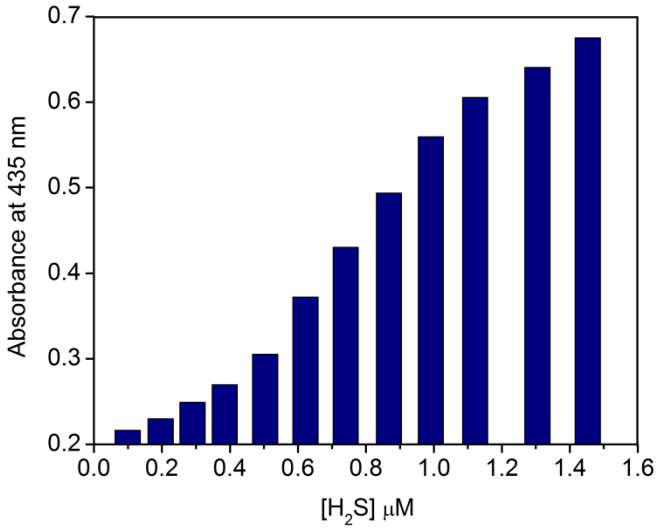

Figure S6. Absorbance plot as a function of concentration of H_2S. The plot implies the enhancement in visual color of the probe solution upon addition of H_2S in CH_3CN/H_2O (1:8, v/v) at pH 7.0.

4. pH titration curve of PN-N_3 upon gradual addition of H_2S:

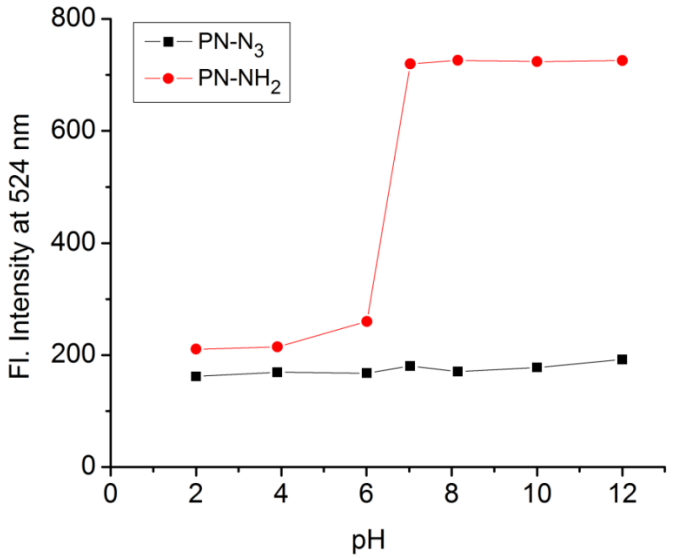

Figure S7. Fluorescence responses of **PN-N_3** (black) and **PN-NH_2** (red) at different pH conditions in CH_3CN/H_2O (1:8, v/v) (λ_{ex}= 435 nm).

5. Calculation of limit of detection (LOD) of PN-N_3 towards H_2S:

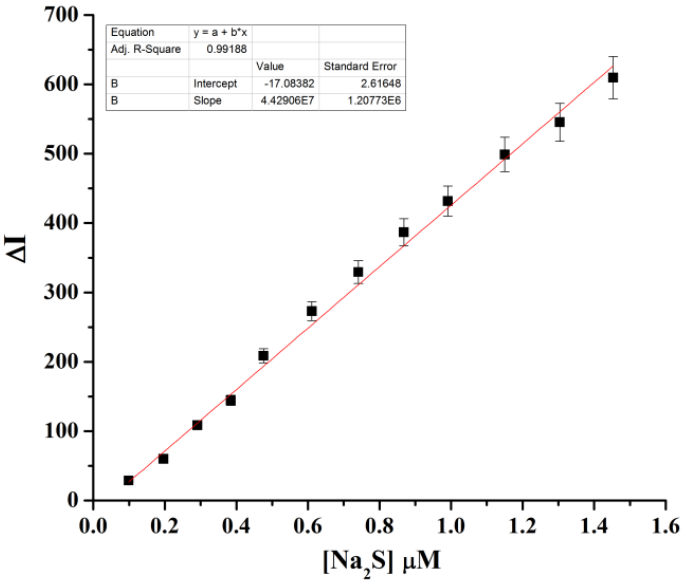

Figure S8. Linear fit curve of **PN-N_3** with respect to Na_2S concentration.

From the linear fit graph of H_2S we get slope = 4.43×10^7, and SD value is 1.46363.
Thus using the above formula we get the Limit of Detection = 66 nM. Therefore, **PN-N_3** can detect H_2S up to this very lower concentration by fluorescence techniques.

6. Job's plot for determining the stoichiometry of interaction by fluorescence method:

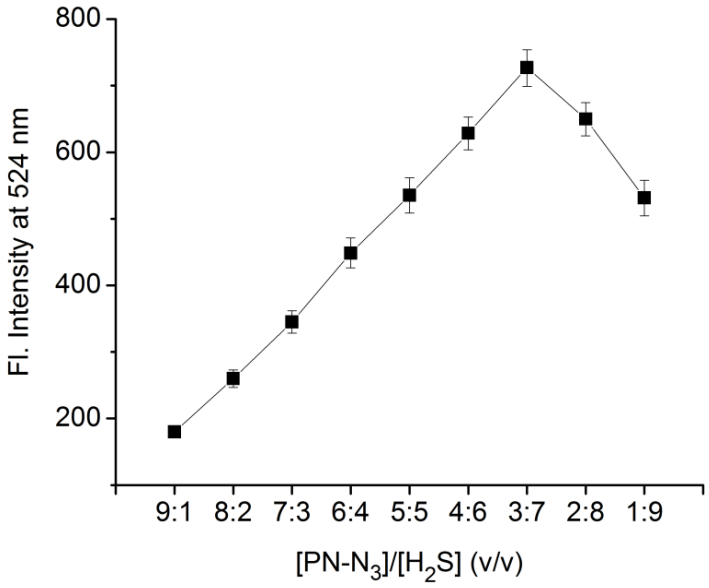

Figure S9. Job's plot of interaction of **PN-N$_3$** with H_2S in acetonitrile-water (1:8, v/v), neutral pH, ([**PN-N$_3$**] = [H_2S] = 10 μM) by fluorescence method (λ_{ex}= 435 nm).

7. Fluorescence response of PN-N$_3$ in liquid and gas phase:

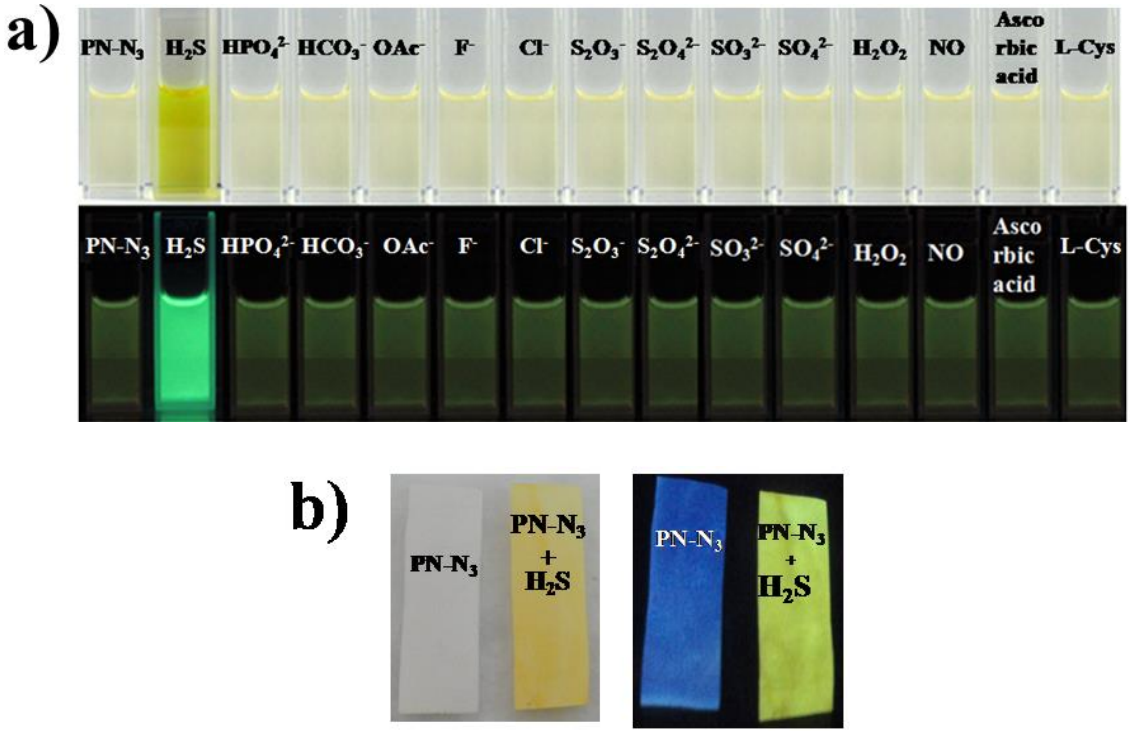

Figure S10. (a) Fluorescence response of **PN-N$_3$** to various anions [From left to right: Only **PN-N$_3$**, **PN-N$_3$** with H_2S, HPO_4^{2-}, HCO_3^-, OAc^-, F^-, Cl^-, $S_2O_3^-$, $S_2O_4^{2-}$, SO_3^{2-}, SO_4^{2-}, H_2O_2, NO, Ascorbic acid and L-cysteine] in acetonitrile–water (1:8 v/v, pH 7.0,10 mM phosphate buffer) solution. (b) Fluorescence color changes visualized on filter paper strips after 10 minutes of incubation of **PN-N$_3$** and **PN-N$_3$** with H_2S respectively.

8. Comparative absorbance and fluorescence titration spectra:

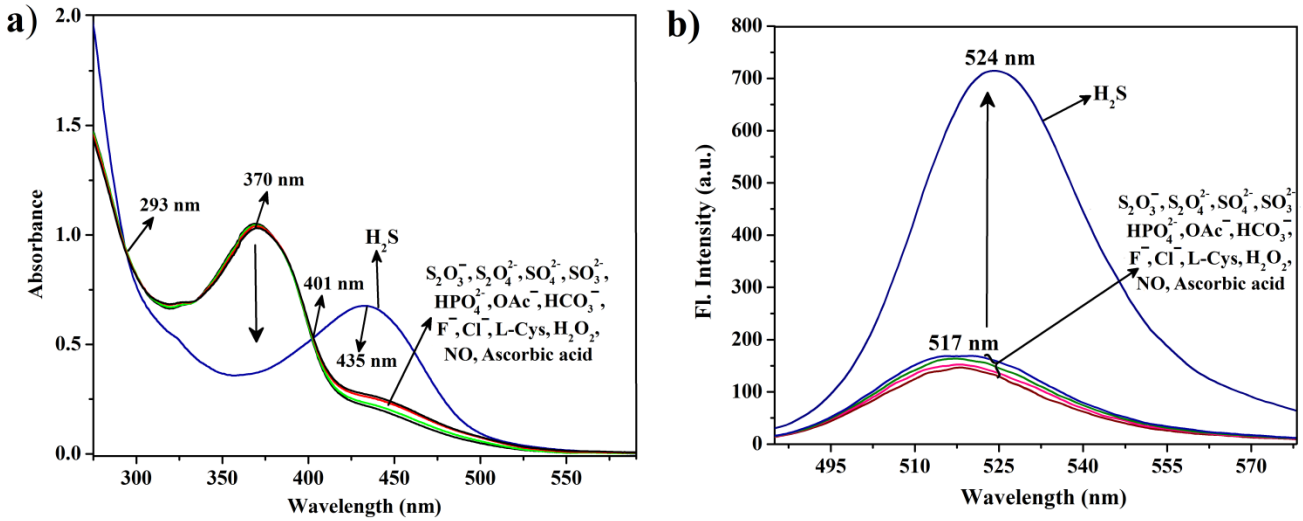

Figure S11. (a) Comparative absorption spectra of **PN-N$_3$** (20 µM) in CH_3CN/H_2O, 1:8 (v/v), (pH 7.0, 10 mM phosphate buffer) after addition of various anions, H_2O_2, NO, Ascorbic acid and L-cysteine, upto 20 equiv. (b) Comparative fluorescence emission spectra of **PN-N$_3$** (c = 20 µM) in CH_3CN/H_2O, 1:8 (v/v), (pH 7.0, 10 mM phosphate buffer) after addition of H_2S along with various anions H_2O_2, NO, Ascorbic acid and L-cysteine up to 20 equiv.

9. ^{1}H NMR titration spectrum of PN-N_3 with H_2S:

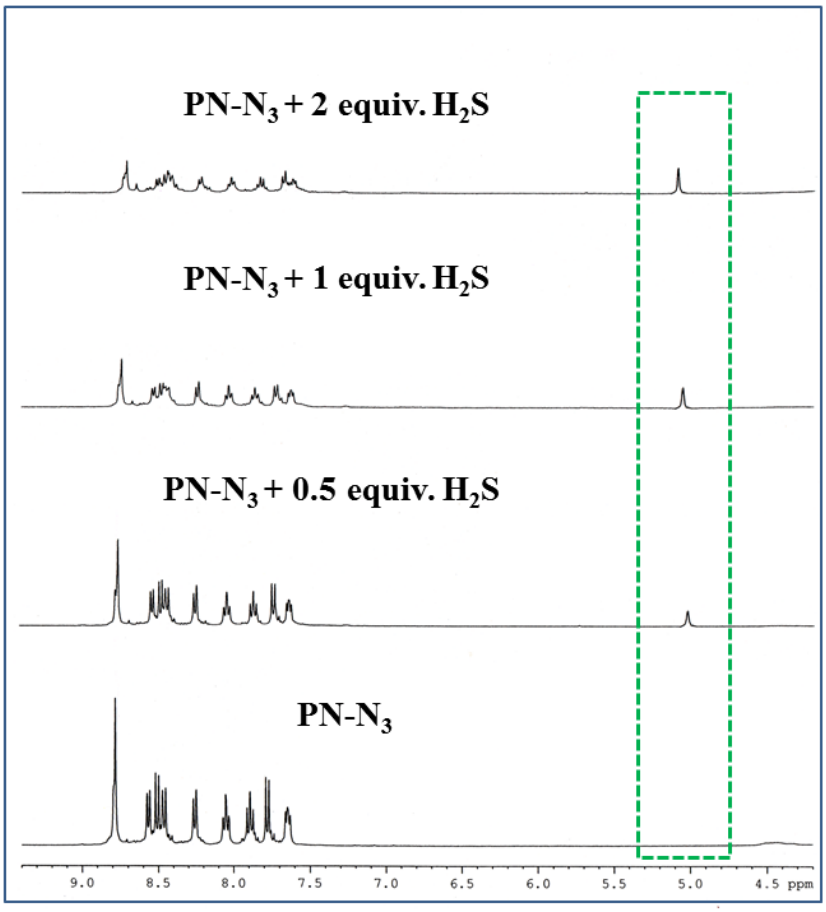

Figure S12. ^{1}H NMR titration spectra [400 MHz] of **PN-N_3** in CD_3CN at 25^0C and the corresponding changes after the gradual addition of one equiv. of H_2S in D_2O from (i) only **PN-N_3**, (ii) **PN-N_3+** 0.5 equiv. of H_2S (iii) **PN-N_3**+ 1 equiv. of H_2S, (iv) **PN-N_3**+ 2 equiv. of H_2S.

10. Partial HRMS of the mixed assay system:

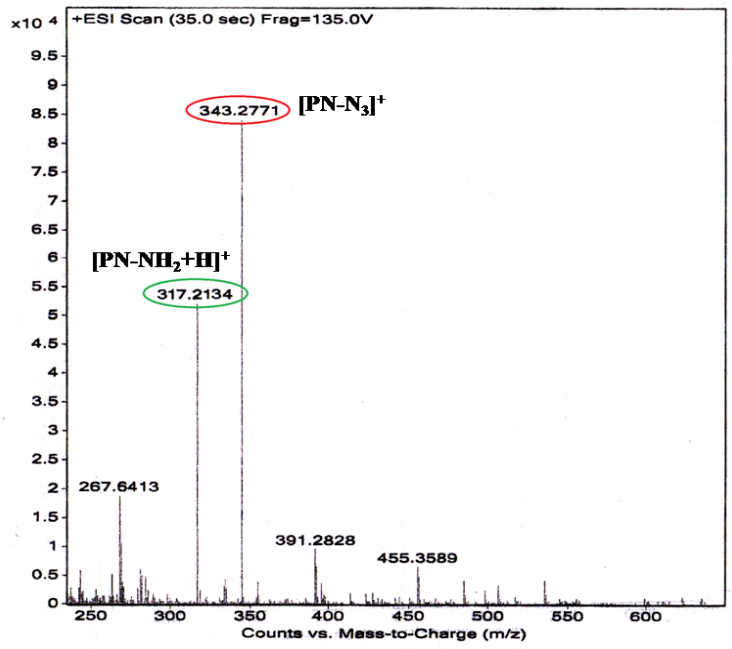

Figure S13. Partial HRMS spectra of **PN-N$_3$**-Na$_2$S mixture in acetonitrile, taken after two hours of mixing.

11. Details of energy calculations using Density Functional Theory (DFT):

Top and side view of energy optimized geometry:

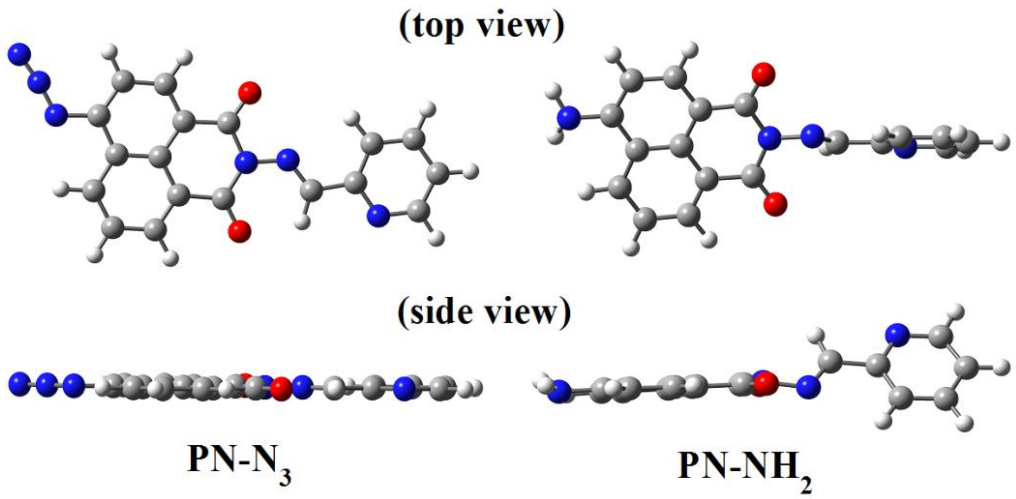

Figure S14. Energy optimized geometries of **PN-N$_3$** and **PN-NH$_2$** obtained at the B3LYP/6-311+G(d,p) levels of theory with CPCM solvation (H_2O).

Table S2. Details of the geometry optimization in Gaussian 09 program.

Details	**PN-N_3**	**1**	**2**	**3**	**PN-NH_2**
Calculation method	RB3LYP	RB3LYP	RB3LYP	RB3LYP	RB3LYP
Basis set	6-311G+(d,p)	6-311G+(d,p)	6-311G+(d,p)	6-311G+(d,p)	6-311G+(d,p)
E(RB3LYP) (a.u.)	-1171.133	-1570.103	-1969.523	-1062.239	-1062.882
Charge, Multiplicity	0, 1	-1,1	0,1	-1,1	0, 1
Solvent (CPCM)	Water	Water	Water	Water	Water

Table S3. Information detailing for the geometry optimization in Gaussian 09 program.

Molecules	**Calculation Method**	**Basis Set**	**E(RB3LYP) (a.u.)**	**Charge, Multiplicity**	**Solvent (CPCM)**
N_2	RB3LYP	6-311G+(d,p)	-109.558	0,1	Water
H_2S_2	RB3LYP	6-311G+(d,p)	-797.638	0,1	Water
HS^-	RB3LYP	6-311G+(d,p)	-398.858	-1,1	Water
H_2S	RB3LYP	6-311G+(d,p)	-399.411	0,1	Water

Table S4. Selected electronic excitation energies (eV), oscillator strengths (f), main configurations of the low-lying excited states of all the molecules and complexes. The data were calculated by TDDFT//B3LYP/6-311G+(d,p) based on the optimized ground state geometries.

Molecules	**Electronic Transition**	**Excitation Energy[a]**	**f[b]**	**Composition[c](%)**
PN-N_3	$S_0 \rightarrow S_1$	3.30 eV at 376 nm	0.8193	H-1→ L+1 (70 %)
	$S_0 \rightarrow S_9$	4.25 eVat 285nm	0.5066	H→ L (69.4 %)
PN-NH_2	$S_0 \rightarrow S_1$	3.09 eV at 408 nm	0.7988	H → L (69.6 %)
	$S_0 \rightarrow S_8$	4.30 eV at 288 nm	0.2219	H-1 → L+1 (68 %)

[a]Only selected excited states were considered. The numbers in parentheses are the excitation energy in wavelength. [b]Oscillator strength. [c]H stands for HOMO and L stands for LUMO.

Table S5. Energies of the highest occupied molecular orbital (HOMO) and lowest unoccupied molecular orbital (LUMO).

Species	E_{HOMO} (a.u)	E_{LUMO} (a.u)	ΔE(a.u)	ΔE(eV)	ΔE(kcal/mol)
PN-N_3	-0.24400	-0.07083	0.17317	4.71	108.66
PN-NH_2	-0.24124	-0.06607	0.17517	4.76	109.90

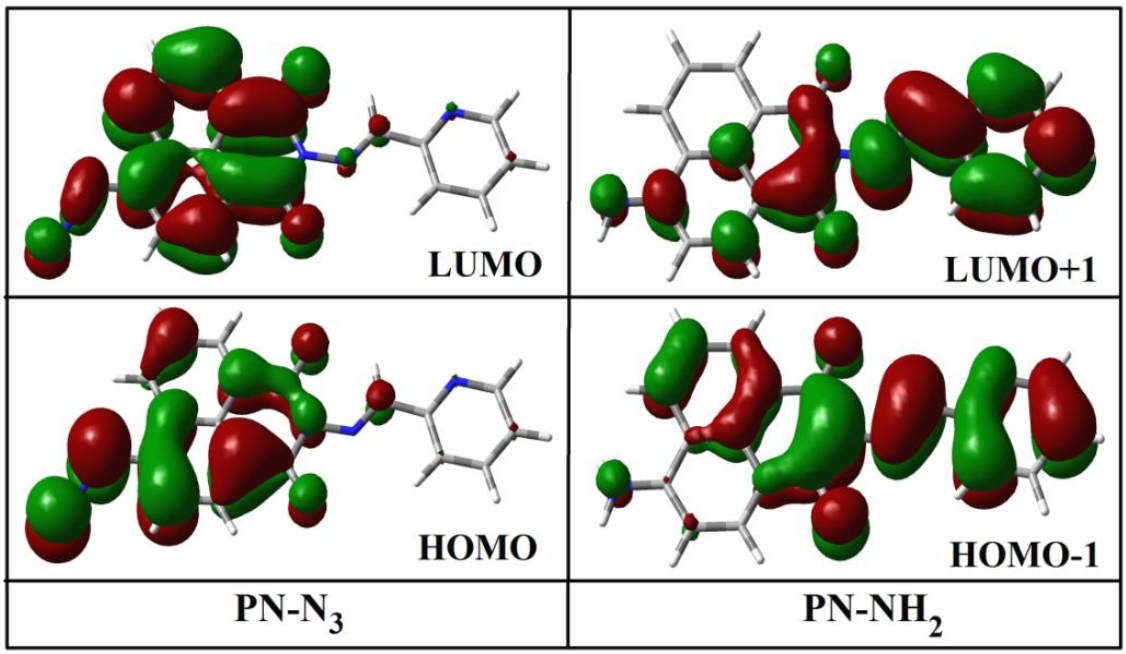

Figure S15. All relevant electronic transitions of the probe **PN-N_3** and the product **PN-NH_2.**

12. Proposed Mechanism:

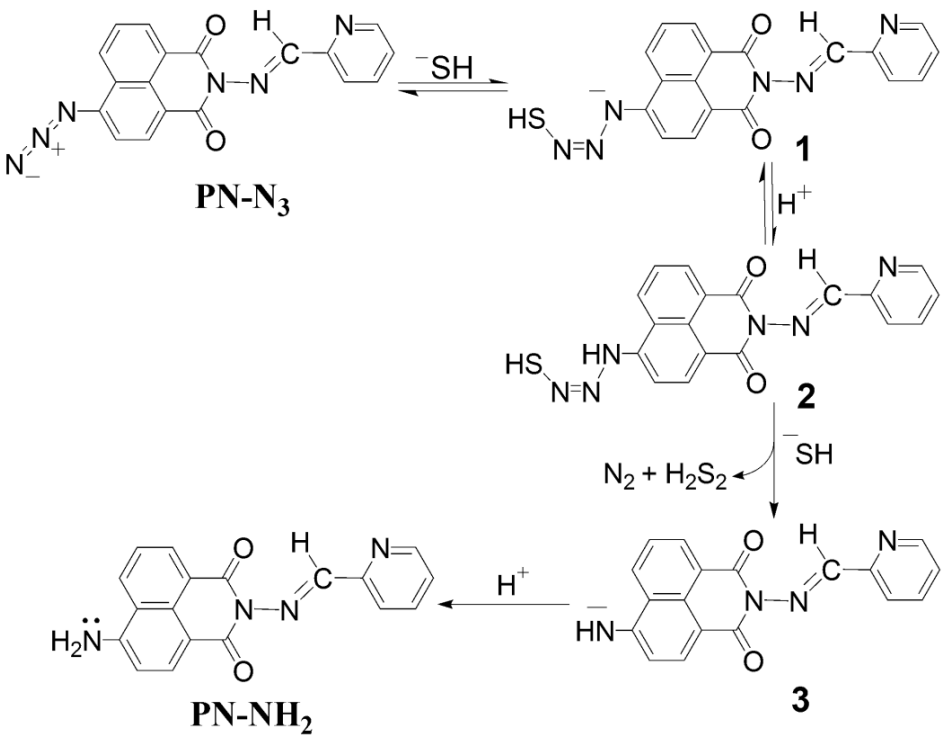

Scheme S1. Proposed mechanism for the formation of **PN-NH$_2$** from **PN-N$_3$** upon addition of two equivalents of H_2S.

13. Images of estimation:

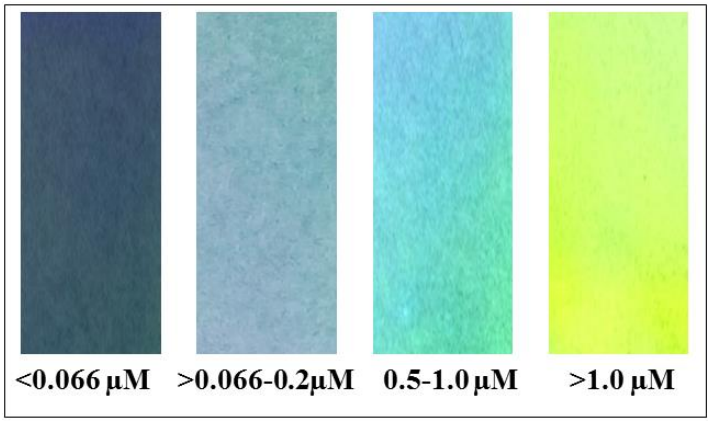

Figure S16. Photographic images of filter paper strips soaked for 1 hour in **PN-N$_3$** and of commercially available Na_2S solution (standard) of different concentrations.

14. Colorimetric assay for the estimation of H_2S:

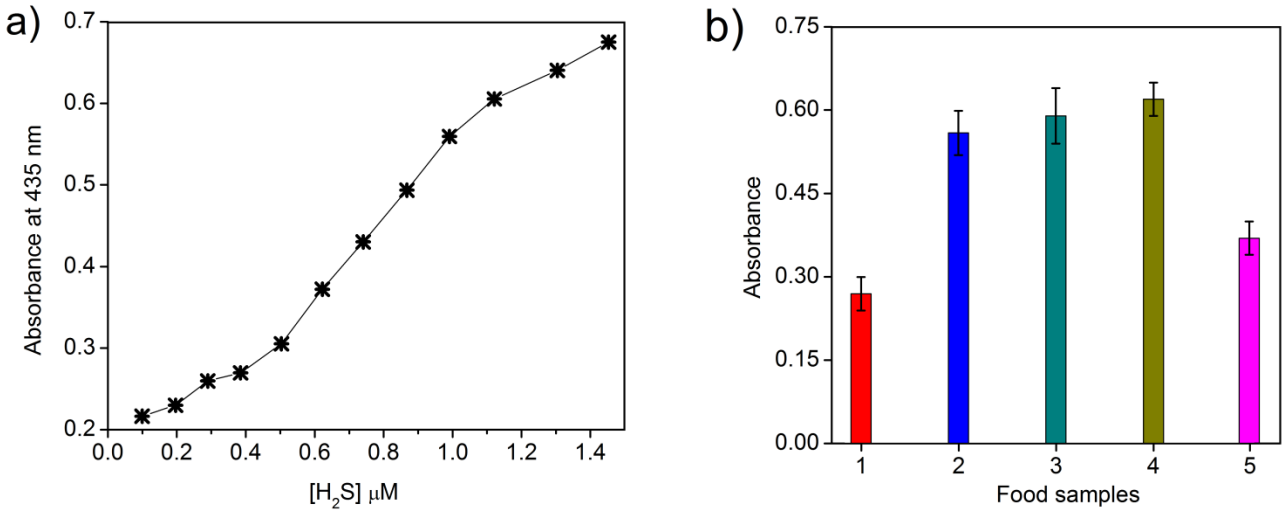

Figure S17. a) Standard absorbance plot for **PN-N3** with varying concentration of H_2S. b) Bar diagram of the colorimetric assay analysis for estimating the concentration of H_2S present in the food samples with the help of standard absorbance plot. Food samples, 1. Soybean; 2. Chicken; 3. Radish; 4. Egg and 5. Cauliflower.